Solid State Communications 152 (2012) 1585–1589

Contents lists available at SciVerse ScienceDirect

Solid State Communications

journal homepage: www.elsevier.com/locate/ssc

Magnetic properties of Co–Cu nanowire arrays fabricated in different conditions by SC electrodeposition

Xiaohui Lin [a], Guangbin Ji [a,*], Tingting Gao [a], Junwu Nie [b], Youwei Du [c]

[a] Department of Applied Chemistry, College of Material Science and Technology, Nanjing University of Aeronautics and Astronautics, Nanjing 211100, PR China
[b] Ningbo Institute of Materials Technology & Engineering, Chinese Academy of Sciences, Ningbo 315201, PR China
[c] Laboratory of Solid State Microstructures, Nanjing University, Nanjing 210093, PR China

ARTICLE INFO

Article history:
Received 30 December 2011
Received in revised form
7 May 2012
Accepted 21 May 2012
by Xianhui Chen
Available online 26 May 2012

Keywords:
A. CoCu nanowire
B. Electrodeposition
C. Magnetic properties

ABSTRACT

Magnetic Co–Cu alloy nanowires with low Cu content were prepared by SC electrodeposition in pores of anodic aluminum oxide templates. The as-deposited Co–Cu nanowires, with a diameter of 15 nm, show distinctive magnetic anisotropy as an applied magnetic field parallel to the axis of nanowires. With increase in the molar ratio of Co and Cu, the coercivity along nanowire axis increases and reaches a maximum value of 1977.5 Oe at the Co/Cu molar ratio of 60:1, but the maximum value of coercivity increases to 1743.6 Oe with the decrease of frequency to 2 Hz.

1. Introduction

Metallic nanowires have attracted wide attention due to their exciting electrical, optical, catalytic, and magnetic properties, with potential applications in optoelectronics [1,2], high-density magnetic memories [3], and sensors [4]. For the applications in perpendicular recording, nanowire is a new promising candidate [5]. Nanowire-based sensors allow for a higher sensitivity, higher capture efficiency, and faster response time due to their large adsorption surface and small diffusion time [6]. Magnetic Cu–Co alloys are known to exhibit giant magnetoresistance (GMR) because of the smaller saturation magnetization and relatively larger giant magnetoresistance effect [7–10]. Chi et al. [11] have fabricated Cu/Co multilayer nanowire arrays and investigated GMR of the samples. There are other investigators studied the magnetic properties and GMR of Co/Cu multilayer flims/nanowires [12–14]. To the best of our knowledge, the microstructures and magnetic properties of the solid solution Co–Cu nanowire arrays have rarely been reported [15].

Among various synthetic processes, the electrodeposition within the nanoporous membranes has been proved to be a promising technique for the preparation of nanowire arrays. Porous anodic aluminum oxide, with high pore density, uniform pore distribution and small diameter of the pores, makes it an ideal template for the fabrication of nanostructured materials [16]. Typically, electrodeposited M–Cu (M=Co, Permalloy, Ni) nanowires are grown using the so-called single bath technique in which a single electrolyte contains both the magnetic and Cu ions and the concentration of Cu ions is quite low [17]. As Co has large magnetocrystalline anisotropy and may be grown with different crystallographic structures, such as cubic or hexagonal, in order to control their specific magnetic properties, the concentration of non-magnetic Cu ions should be low during the electrodeposition procedure. It has been shown that nearly pure magnetic layers could be obtained by keeping the Cu concentration very low ($<2\%$) [18]. In this paper, by keeping the Cu concentration lower than 10%, Co–Cu nanowires grown into porous anodic aluminum oxide templates were successfully fabricated via electrodeposition with square-wave voltages. The magnetic properties of the nanowire arrays with different molar ratio of Co/Cu (10:1, 20:1, 40:1, 50:1, 60:1) were widely investigated. The frequency of voltage which is a key factor of electrodeposition and the influence of voltage were studied as well.

2. Experiment

Nanoporous anodic aluminum oxide (AAO) templates were prepared by the process described previously [19]. The anodizing process was carried out at $\sim 0\ ^\circ C$ with H_2SO_4 as electrolyte for 6 h, and the DC anode voltage is 10 V. All the templates were immersed in 0.3 M H_3PO_4 for 5–10 min to dissolve the oxide layer, and then

* Corresponding author. Tel.: +86 25 52112902; fax: +86 25 52112626.
E-mail address: gbji@nuaa.edu.cn (G. Ji).

0038-1098/$ - see front matter
http://dx.doi.org/10.1016/j.ssc.2012.05.016

washed by distilled water. The Co–Cu nanowires were electrodeposited into the pores by square-wave pulse current (SC) electrolysis in an electrolyte consisting of $Co(Ac)_2 \cdot 4H_2O$ (1 mol/L), $CuSO_4 \cdot 5H_2O$ (0.1, 0.05, 0.025, 0.02 and 0.017 mol/L), and H_3BO_3 (10 g/L). SC electrodeposition was conducted at 20–26.9 V with a frequency of 25 Hz at room temperature, and the duty cycle was set as 50%. Moreover, another series of electrodeposition were conducted at different frequency (2, 10, 25, 50, 100, 150 and 200 Hz) with the constant Co/Cu ratio of 50:1. The bottom aluminum layer was removed in $CuCl_2$ solution, and the nanowires were released from the AAO templates by NaOH solution. The as-deposited nanowires gained from the electrolyte with different CoCu ratios were denoted as *Rn* ($n=10$, 20, 40, 50, 60), here "*R*" is an abbreviation for "ratio", "*n*" represents for the different CoCu ratio of electrolyte. And for the nanowires deposited at different frequencies of voltage, they were denoted as *Fn*, here "*F*" is an abbreviation for "frequency", "*n*" represents for the value of frequency.

The obtained nanowires were characterized by field emission scanning electron microscopy (FE-SEM, Hitachi S-4800) and transmission electron microscopy (TEM, JEOL JEM-2100). The crystal structures of the nanowire arrays embedded within AAO templates were examined by using an X-ray diffractometer (XRD, Bruker D8 ADVANCE), and the magnetic properties of the samples were measured by a vibrating sample magnetometer (VSM, Lakeshore, Model 7400 series).

3. Results and discussion

3.1. Characterization of the Co–Cu nanowires

Fig. 1 shows the SEM and TEM images of the Co–Cu nanowires. Fig. 1(a) reveals that the nanowires with a length of ~3 μm are well-aligned and orderly along one direction. From the top view, it can be seen that the nanowires arrays congregate to some bundles in areas without the dependence of AAO template, and this may attribute to the magnetic force between nanowires and the specific surface energy caused by the high surface area of nanowires. Fig. 1(b) shows an enlarged SEM image of Co–Cu nanowires, and it is clear that the nanowires of a diameter of ~15 nm are highly parallel to each other and uniform throughout the whole length which mainly depends on the well-ordered nanochannels of the AAO templates. Some particles have been found to attach to the surface of nanowire which may be induced by the residual AAO template after dissolving by NaOH solution. The broken nanowires also can be seen from Fig. 1(b), which

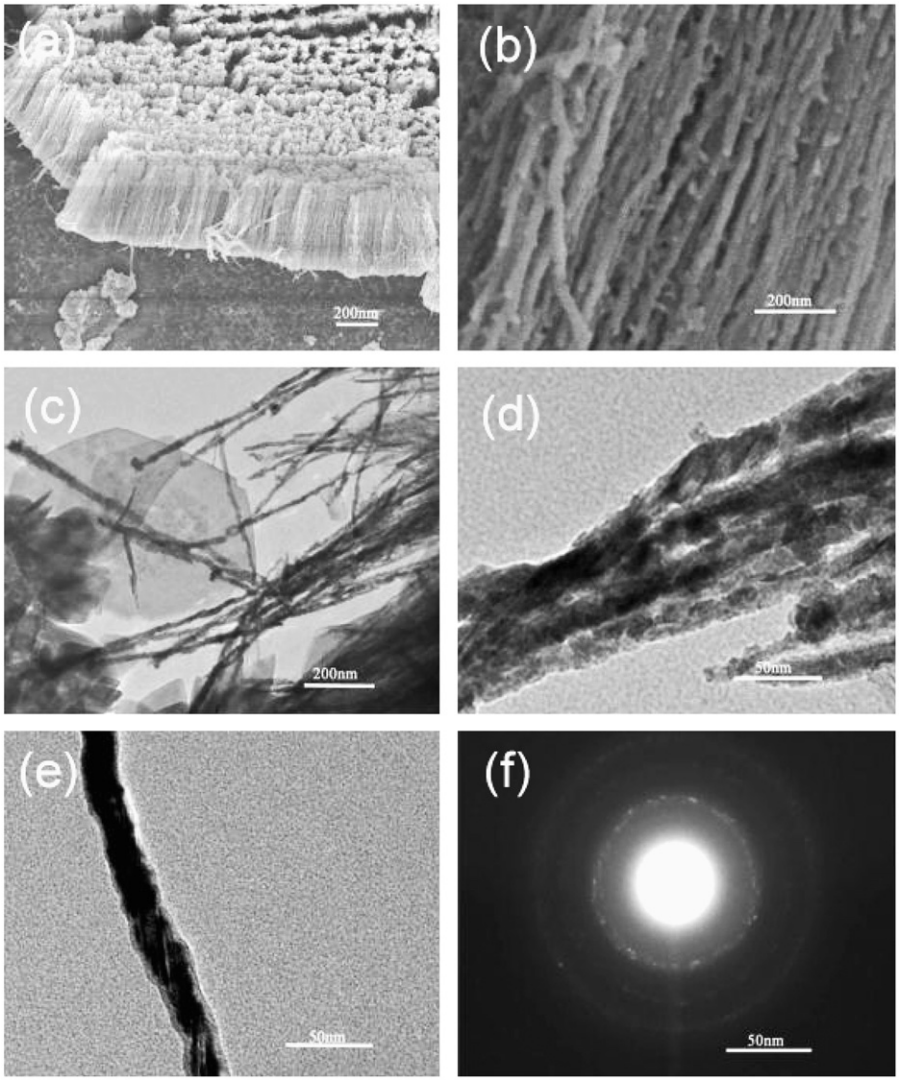

Fig. 1. FE-SEM images of Co–Cu nanowires (a, b); TEM images of Co–Cu nanowires (c, d, e, f).

caused by two main reasons: the defects of AAO template and the electrodeposition progress. Fig. 1(c, d, e, f) show the TEM images of Co–Cu nanowires which have been released from the AAO templates. From Fig. 1(c), it also illustrates that the lengths of all the nanowires are larger than 2 μm, and the nanowires are continuous with a uniform diameter throughout their entire length. In some regions, amounts of nanowires arranged along one direction and parallel to each other which was contributed to the arrangement of channels of AAO template. The semitransparent sheets around the nanowires were probably the undissolved template. Fig. 1(d) gives the enlarge image of few nanowires, and it can be seen that the wires gathered and several intensive growth parts appeared in the single nanowire which often occurred in electrodeposition. During the electrodeposition process, even a small change to the parameters such as voltage, current density and concentration of electrolyte will affect the components and structure of nanowires. Fig. 1(e) shows a single nanowire with a diameter of about 15 nm and the length of 2 μm, the aspect ratio of the nanowire can be easily gotten from the image which should be over 100. The edge of the nanowire is not smooth and straight enough because of the imperfection of the AAO template. The aluminum used for anodization and the operating temperature are the two main factors which decide the morphology of AAO template, therefore the incomplete annealing of aluminum and the increase of temperature both will result in the imperfect nanochannels of AAO templates. The diffraction spot of Co–Cu nanowires is shown in Fig. 1(f), few bright spots can be seen in the image. Although they are not obvious which due to the weak crystallization of Co–Cu nanowires, it can prove the nanowires are polycrystalline.

3.2. *The effect of molar ratio of CoCu electrodeposition solution on nanowires*

Fig. 2 shows the XRD patterns of the nanowire arrays which deposited at the Co/Cu ratio of 50:1 and 10:1. There are two diffraction peaks corresponding to the fcc (111) and (101) plane of Co at the 2θ of 44.3° and 47.6°, respectively, which means the grains grow along Co (111) and Co (101) crystal directions, and the preferential orientation of the nanowires may attribute to the confined growth of the nanowires within the porous alumina film.

The magnetic properties of the nanowires synthesized with different Co/Cu ratio are shown in Fig. 3. Fig. 3(a) shows the

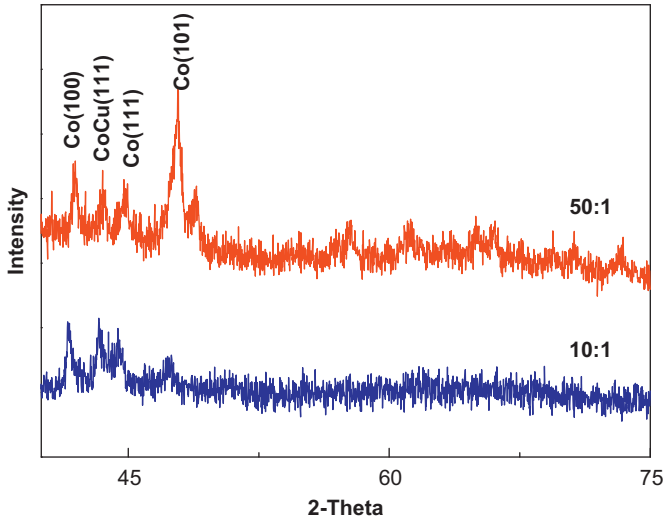

Fig. 2. (Color online) XRD pattern of as-synthesized Co–Cu nanowires with the deposited Co/Cu at the ratio of 50:1 and 10:1.

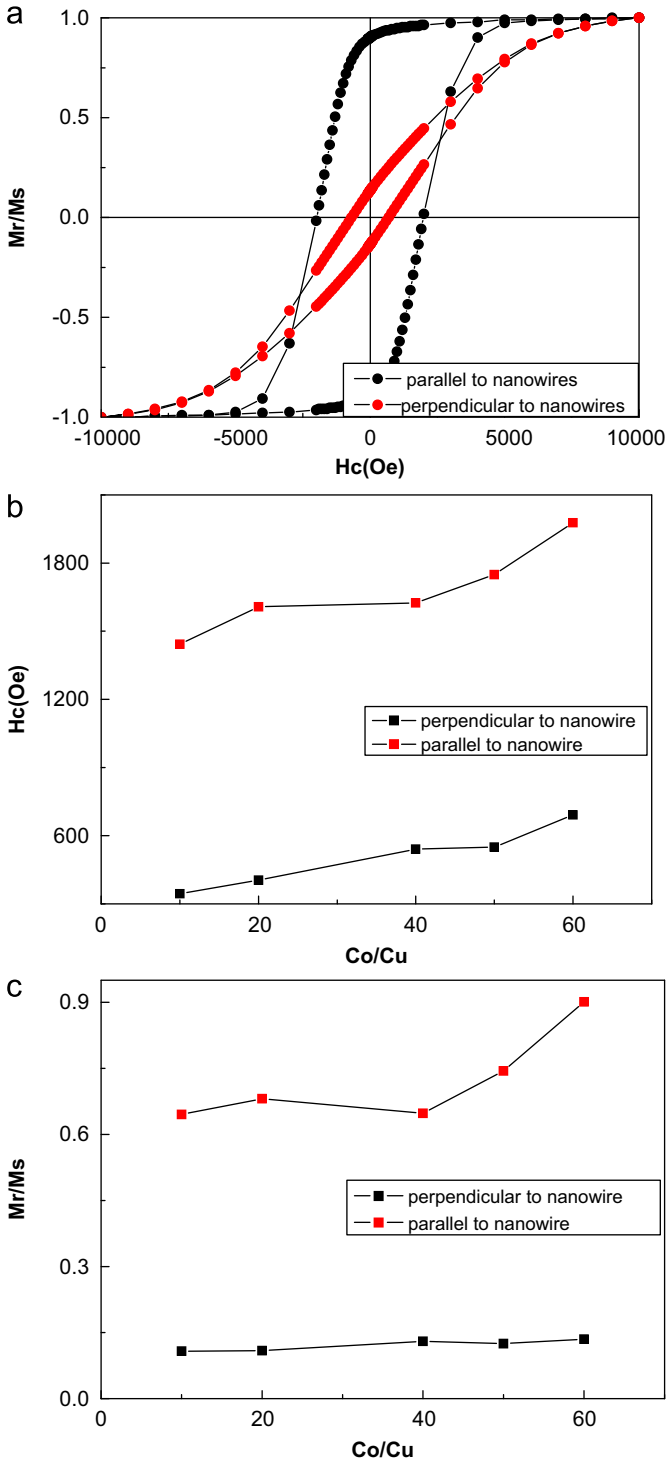

Fig. 3. (Color online) The typical hysteresis loop of the nanowires synthesized with Co/Cu ratio at 60:1 (a); the change in Hc, $Hc_{//}$ (b); and squareness (Mr/Ms) (c) of the nanowires versus the Co/Cu ratio of the electrolyte.

hysteresis loop of the nanowires synthesized with Co/Cu ratio of 60:1. It is found that the nanowires possess shape anisotropy and the easy magnetic axis parallel to the axis of the nanowires. The change in $Hc_{\perp}$ and $Hc_{//}$ of the nanowires as a function of Co/Cu ratio of the electrolyte are shown in Fig. 3(b, c). In the process of electrodeposition, with the increase in the proportion of Co–Cu, the content of Co increases. In the Co–Cu alloy, the magnetism of the nanowires is mostly determined by the Co. Therefore, the higher content of Co will contribute to the larger influence of

magnetism. From the figures we can see that both *Hc* ($Hc_{//}$ and $Hc_{\perp}$) and squareness (*Mr*/*Ms*) of the Co–Cu nanowires are enhanced with the increase in Co/Cu ratio of the electrolyte and maximum value of coercivity (1977.5 Oe) and squareness (0.92) can be achieved at Co/Cu ratio of 60:1. Saturation magnetization increases with the increase of Co content in the system, so the shape anisotropy energy (Edemag$=\pi Ms^2$) also increases, which leads to the enhancement of energy barrier during magnetization reversal. As a result, the coercivity is enhanced with the increase of Co content.

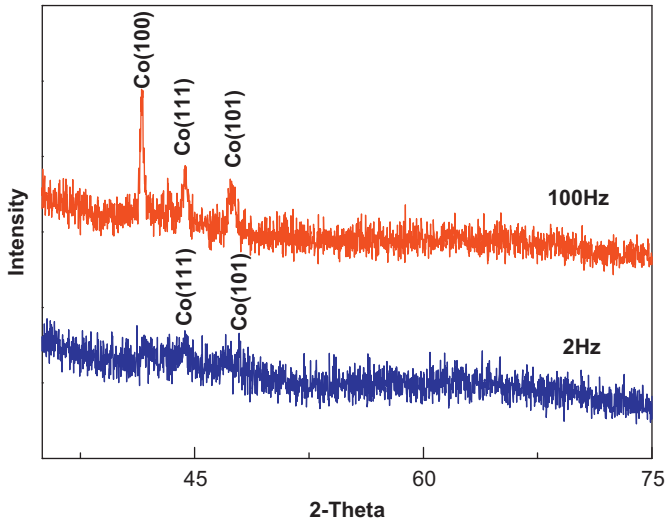

Fig. 4. (Color online) XRD pattern of nanowires wires with different supply frequency.

3.3. The effect of frequency on nanowires

Fig. 4 shows the XRD patterns of as-synthesized Co–Cu nanowires under different supply frequency with the Co/Cu ratio of 50:1. It is found that the nanowire arrays are mainly Co crystalline phase. The diffraction peaks corresponding to the (100), (111) and (101) plane of Co can be observed at the 2θ of 41.5°, 44.3° and 47.6° respectively in 100 Hz. While the Co crystalline phase structure obtained in 2 Hz is not obvious, which means that there are no typical diffraction peaks of CoCu alloy.

A typical hysteresis loop of the nanowires synthesized at the frequency of 2 Hz (a) is shown in Fig. 5(a). From Fig. 5(b), it can be found that the *Hc* of the nanowires decreased by increasing the supply frequency when they are parallel to the applied magnetic field, however, the values of the $Hc_{//}$ are kept constant when the supply frequency is above 50 Hz. This tendency may be caused due to the change in Co content. Meanwhile, the *Hc* can be influenced by intergranular exchange coupling interactions. In lower frequency electric deposition, the influence of Co content on *Hc* plays a leading role, with the increase of the frequency, the

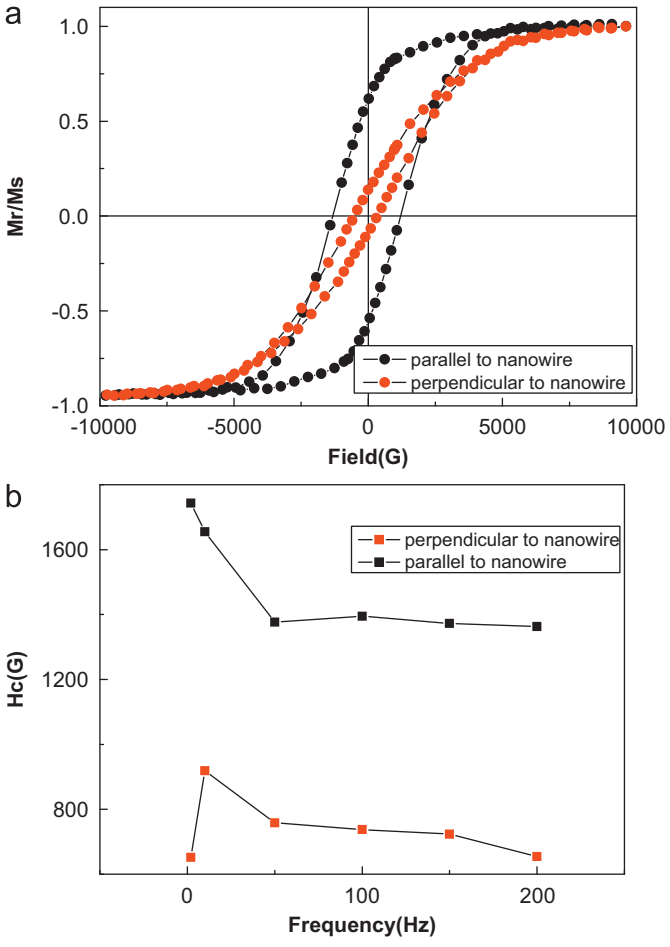

Fig. 5. (Color online) The typical hysteresis loops of the nanowires synthesized at the frequency of 2 Hz (a); and the variation tendency of *Hc* on frequency of electrodeposition (b).

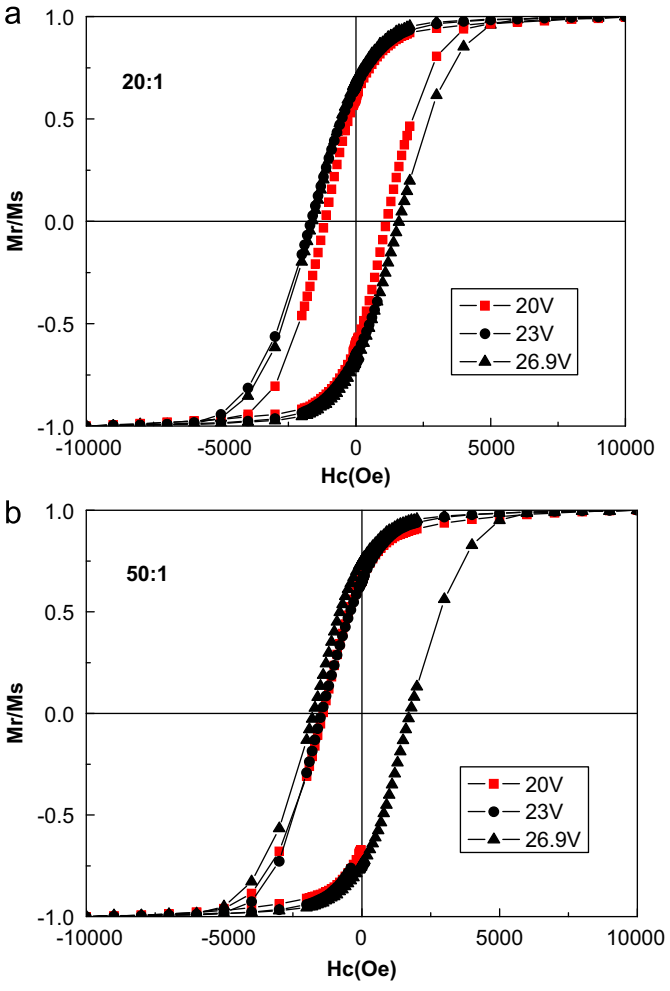

Fig. 6. (Color online) The hysteresis loops of the nanowires synthesized at different voltages at the electrolyte with different Co/Cu ratio.

grain may be changed, and the effect of exchange coupling interaction should be considered. From Fig. 5, one can see that the *Hc* reached the maximum value at 10 Hz, when the magnetic field perpendicular to the axis of the nanowires.

3.4. The effect of voltage on magnetic properties of the nanowires

As compared to direct voltage deposition, the influence of alternating voltage and square-wave voltage on the deposition of nanowires may not be so distinct. In order to investigate the effects on the magnetic properties of the nanowires, three different applied voltages (20, 23 and 26.9 V) have been selected. For the electrolyte with different Co/Cu proportion (20:1 and 50:1), it is obvious that with the increase in voltage, some changes can be found for the values of *Ms* and *Hc* as shown in Fig. 6. The reasons for the changes can be attributed to the different voltages lead to produce different Co and Cu precipitation amounts. It is well known that the electrochemical potential of Co^{2+} is higher than Cu^{2+}, so in the lower voltage, the deposition rate of Cu^{2+} is faster than Co^{2+}. On the contrary, the deposition rate of Co^{2+} is faster. As a result, with the increase in voltage, the precipitation amount of Co is more than Cu.

4. Conclusion

Magnetic Co–Cu alloy nanowires were successfully grown in small pore size AAO templates by SC electrodeposition. The nanowires have polycrystalline structure, showing clearly magnetic anisotropy with the preferred magnetization direction parallel to the axis of nanowires. Both the coercivity and squareness of Co–Cu nanowires increased with the increase of Co/Cu ratio in electrolyte and fairly large coercivity (1977.5 Oe) and squareness (0.92) can be achieved. On the other hand, the coercivity decreased with the frequency of power and kept constant when the frequency was higher than 50 Hz, and this result was the combined action between the content of Co deposited in nanowires and the exchange coupling effect.

Acknowledgments

Support by the Aeronautics Science Foundation of China (2011ZF52064), National Natural Science Foundation of China (51172109) and Natural Science Foundation of Jiangsu Province of China (no.: BK2010497) is gratefully acknowledged.

References

[1] T. Yanagishita, K. Nishio, H. Masuda, Appl. Phys. Express 1 (2008) 067004.
[2] H. Masuda, M. Ohya, H. Asoh, M. Nakao, M. Nohtomi, T. Tamamura, Jpn. J. Appl. Phys. Part 2: Lett. 38 (1999) L1403.
[3] G.B. Ji, J.M. Cao, F. Zhang, G.Y. Xu, H.L. Su, S.L. Tang, B.X. Gu, Y.W. Du., J. Phys. Chem. B 109 (36) (2005) 17100.
[4] M.S. Gabureac, L. San Emeterio Alvarez, C.H. Marrows, Procedia Chem. 1 (2009) 851.
[5] J. Cho, J. Min, S. Ko, J. Appl. Phys. 99 (2006) 08C909.
[6] E.C. Walter, F. Favier, R.M. Penner, Anal. Chem. 74 (2002) 1546.
[7] C. Meneghini, S. Mobilio, A. Garcia-Prieto, M.L.F. Fdez-Gubieda, Nucl. Instrum. Methods B 200 (2003) 215.
[8] M.G.M. Miranda, A.T. da Rosa, M.N. Baibich, E. Estevez-Rams, G. Martinez, Phys. Rev. B 354 (21) (2004) 88.
[9] G. Martinez, M.N. Baibich, M.G.M. Miranda, E. Vargas, J. Magn. Magn. Mater. 272–276 (2004) 1716.
[10] O. Karaagac, M. Alper, H. Kockar, J. Magn. Magn. Mater. 322 (2010) 1098.
[11] G.J. Chi, Z.Y. Feng, J. Zhou, S.W. Yao, Acta Phys. Chim. Sin. 19 (2) (2003) 177.
[12] D. Rafaja, C. Schimpf, T. Schucknecht, V. Klemm, L. Peter, I. Bakonyi, Acta Mater. 59 (8) (2011) 2992.
[13] B.G. Toth, L. Peter, I. Bakonyi, J. Electrochem. Soc. 158 (11) (2011) D671.
[14] D.L. Khalyapin, P.D. Kim, J. Kim, I.A. Turpanov, A.Ya. Beten'kova, G.V. Bondarenko, T.N. Isaeva, I. Kim, Phys. Solid State 52 (9) (2010) 1787.
[15] T. Wang, F.S. Li, Y. Wang, L.J. Song, Phys. Status Solidi A 203 (10) (2006) 2426.
[16] P.H. Zhou, D.S. Xue, H.Q. Luo, J.L. Yao, H.G. Shi, Nanotechnology 15 (2004) 27.
[17] L. Piraux, J.M. George, J.F. Despres, C. Leroy, E. Ferain, R. Legras, K. Ounadjela, A. Fert, Appl. Phys. Lett. 65 (1994) 2484.
[18] A. Blondel, J.P. Meier, B. Doudin, J.P. Ansermet, Appl. Phys. Lett. 65 (1994) 3019.
[19] X.H. Lin, G.B. Ji, T.T. Gao, X.F. Chang, Y.S. Liu, H.Q. Zhang, Y.W. Du, Solid State Commun. 151 (2011) 1708.